Reducing drifting Fish Aggregating Devices number and impacts through cooperation

Amaël Dupaix [1,2,3], Patrice Guillotreau[1], Jean-Louis Deneubourg[2], Manuela Capello[1], & Laurent Dagorn[1]

[1] MARBEC, Univ. Montpellier, IRD, Ifremer, CNRS – Sète, France
[2] CENOLI, Université Libre de Bruxelles – Bruxelles, Belgium
[3] Laboratoire de Biologie des Organismes et des Écosystèmes Aquatiques-BOREA, Muséum national d'Histoire naturelle (MNHN), SU, CNRS, IRD, UA, F-75005 Paris, France

Correspondence: amael.dupaix@mnhn.fr

Abstract

Drifting fish aggregating devices (FADs), equipped with echosounder buoys, are highly effective tools that significantly enhance tuna catchability for purse seine vessels. However, FADs are also responsible for various ecological impacts - some well established, others still debated within the scientific community. These ecological impacts highlight the need to develop strategies aimed at reducing FAD numbers. In this study, we explore the potential of buoy information sharing among vessels as a means to reduce FAD numbers while maintaining purse seine fleets profitability. By developing an Individual-Based Model, built upon a pelagic species behavioral model, we demonstrate that FAD numbers in the Indian Ocean could be reduced by 75 % through coordinated information sharing. This reduction not only improves vessel profitability by cutting private costs and increasing revenue, but also strongly decreases social costs, such as carbon emissions and FAD stranding. However, this approach also highlights trade-offs, as it leads to a slight increase in silky shark bycatch. Therefore, careful consideration will be required to balance these outcomes and guide future FAD management strategies.

Keywords: Individual-based model; Echosounder buoys; Stranding; Bycatch; Private and social costs; Equity; Purse seine

1 Introduction

Purse seine (PS) fisheries targeting tropical tuna started to deploy drifting Fish Aggregating Devices (FADs), and to attach radio buoys to them in the 1980s, to facilitate the search and capture of tunas (Ariz et al., 1999; Hall, 1992; Hallier and Parajua, 1999; Marsac, Fonteneau, and Michaud, 2014). Since then, the use of FADs sharply increased (Dagorn et al., 2013; Gershman et al., 2015; Maufroy et al., 2017). A recent study estimated the number of FADs deployed yearly at the global scale to be between 116,000 and 140,000 per year since 2015 (Schiller et al., 2025). This would represent a total of around 1.41 million FADs deployed between 2007 and 2021.

FADs are highly efficient fishing tools that increase tuna catchability, leading PS fleets to extend their fishing zones and preferentially targeting schools associated to floating objects (Fonteneau et al., 2015; Lennert-Cody et al., 2018; Lopez et al., 2014; M Tolotti et al., 2022). In 2017-2021, more than 40 % of global purse seine catch of tuna came from associated schools (ISSF, 2023). During the last two decades, echosounder buoys have replaced radio buoys that were initially associated with FADs. These echosounder buoys transmit GPS data and rough estimates of aggregated biomass under FADs directly to fishing vessels via satellite, significantly lowering search costs and increasing harvest efficiency (Lopez et al., 2014; Tidd, Floc'h, et al., 2023; Wain et al., 2021).

The massive increase in the use of FADs since the 1980s has several potential ecological impacts, which can be decomposed into three main categories. First, a lot of FADs are left adrift and end up stranding on coastal reefs or beaches, causing damage to coastal habitats (Escalle, Mourot, et al., 2023; Escalle, Phillips, et al., 2019; Imzilen, Lett, Chassot, and Kaplan, 2021; Imzilen, Lett, Chassot, Maufroy, et al., 2022). Then, FADs can also impact non-targeted pelagic species, either through ghost fishing (via the entanglement in the nets that constitute their structure) and/or bycatch (Filmalter et al., 2013; Gilman, 2011). Finally, FADs can impact target species, tropical tuna, either by increasing fishing efficiency - potentially leading to overfishing - or by altering their habitat through their presence at the ocean surface (Dupaix, 2023). There is no scientific consensus on some of these impacts, and even for those that are generally agreed upon, their extent remains uncertain. For example, although it was demonstrated that FADs significantly modify the habitat of pelagic species (Dupaix, Capello, et al., 2021; Dupaix, Dagorn, et al., 2024), the fact that these modifications could attract and/or retain tuna in areas that are detrimental to them (the *ecological trap* hypothesis) is still very much debated (Dupaix, Ménard, et al., 2024; Marsac, Fonteneau, and Ménard, 2000).

Although FAD impacts and their extent remain subject to debate, solutions are necessary if we aim to reduce their use. This study is based on the premise that we want to reduce the number of FADs, therefore reducing their potential and actual ecological impacts. Hence, we assess how the number of FADs can be reduced without impacting those using these tools, *i.e.* without impacting the economic results of purse seine fleets. We investigate vessel cooperation as a strategy to reduce the number of FADs and their environmental impacts. This cooperation is based on information sharing, specifically as we analyze the effects of sharing data from echosounder buoys associated to FADs. Developing an Individual-Based Model of a purse seine fleet, built upon a behavioral model of tuna around FADs, we design multiple scenarios to evaluate the effects of information sharing on purse seine fleets' private and social costs.

2 Material and methods

2.1 Individual based model

A spatial Individual-Based Model (IBM) was constructed to simulate the fishing behavior of purse seine (PS) vessels in an array of Fish Aggregating Devices. In the model, purse seine vessels are considered to fish only on FAD-associated schools. FADs are distributed randomly in space and each of them is equipped with an

active echosounder buoy, giving information on FAD position and tuna presence/absence at FAD to the vessels that follow the buoy. In real PS fleets, vessels deploy their FADs equipped with echosounder buoys, which are previously activated *i.e.*, satellite connections are established, allowing the buoy to remotely transmit its position and the associated biomass indices detected nearby the FAD. These echosounder buoys can be deactivated remotely *i.e.*, satellite communications can be remotely interrupted and no more information is transmitted to the vessels. In the Indian Ocean, it was shown that for an average of 10,700 active buoys followed on a daily basis in 2020-2023, around 25,000 FADs were deployed (IOTC, 2024). Hence, it is important to note that, although they are closely linked, the set of active buoys in our model does not correspond to the total number of FADs at sea nor to the total number of FADs deployed, but to the daily number of active echosounder buoys.

2.1.1 FAD occupancy by tuna

Each FAD can be either occupied by tuna (F_o) or empty (F_e) and its occupancy is randomly picked at the initialization. Then, it alternates periods of continuous occupancy (aggregation Continuous Residence Times, aCRTs) and continuous emptiness (aggregation Continuous Absence Times, aCATs; Baidai et al., 2020a). To obtain aCRT and aCAT values, acoustic data collected by Marine Instruments M3I buoys, in 2020-2021 in the Indian Ocean, were translated into presence/absence of a tuna aggregation, using a machine learning algorithm (Baidai et al., 2020b). This algorithm was shown to provide good accuracy (85 %) in the Indian Ocean. In M3I buoys data, the first sections of presence or absence occurring at the beginning of the FAD trajectories were excluded from the analysis. These sections may result from the colonization period of the FAD during which the FAD-tuna system is not yet at equilibrium, or potentially from classification errors related to the operation on the buoy (Baidai et al., 2020b). Presence/absence data was used to obtain aCRT and aCAT distributions.
To account for the impact of FAD density on FAD occupancy, we used the non-social model from Capello et al., 2022. We calibrated this model using data from Govinden et al., 2021 and Dupaix, Dagorn, et al., 2024, allowing to determine the relationship between FAD density and average aCAT, aCRT and aggregation size (m) values (see Supplementary S1). For each simulation, aCAT and aCRT distributions were estimated to set the average value to the one obtained from the model (Figure S1). For the system to reach equilibrium before the simulations, vessels were released in the system 100 days after initialization (Figure S2).

2.1.2 Vessel behavior

We note F the set of all the echosounder buoys distributed randomly in the model ($F = [1; n]$, with n the number of elements in F). We consider that each vessel receives information from a given set of buoys (followed FADs, noted F_f). For each vessel i, the set of all the echosounder buoys present in the system can be divided as follows:

$$F = F^i_{o,f} \cup F^i_{o,u} \cup F^i_{e,f} \cup F^i_{e,u} \tag{1}$$

where $F^i_{o,f}$ are the FADs occupied by tuna and followed by vessel i, $F^i_{o,u}$ the FADs occupied by tuna and not followed by vessel i, $F^i_{e,f}$ the FADs not occupied by tuna followed by vessel i, and $F^i_{e,u}$ the FADs not occupied by tuna and not followed by vessel i. With this definition, the intersections of the four above-mentioned subsets of F are empty (*e.g.* $F^i_{o,f} \cap F^i_{o,u} = \varnothing$).
Each vessel can be in 4 different states: (1) *traveling*, (2) *fishing*, (3) *resting* and (4) *idle* (Figure 1). When a vessel is *traveling*, it goes at a constant speed in a straight line towards the closest FAD that is occupied by tuna and for which it has the information of tuna presence. This information can be obtained by the vessel in two ways: either the vessel receives the buoy information from the FAD or the FAD is at less than a given detection radius (R), allowing the vessel to detect tuna presence using a bird radar. Hence, the aim FAD (the FAD towards which the vessel orients itself) of vessel i is the FAD j such that:

$$\begin{cases} j \in F_A^i \quad \text{with} \quad F_A^i = F_{o,f}^i \cup \{k \in F_{o,u}^i \text{ with } d(i,k) \leq R\} \\ d(i,j) = \min_{l \in F_A^i} d(i,l) \end{cases} \tag{2}$$

where $d(i,l)$ is the distance between vessel i and FAD l and F_A^i the set of all the FADs available to be fished by vessel i. Notice that the second term in Eq. 2 implies that if multiple FADs are available to the vessel, it heads towards the closest one. When the vessel reaches the aim FAD, if it's the day it starts *fishing*, if it's the night it waits for the following day to start fishing (*resting* state). Day and night duration were considered to last 12 h each.

When *fishing*, the vessel stays at the FAD for a given duration. This duration corresponds to the duration of a fishing set (t_s) and was obtained using data from observers onboard French purse seine vessels in the Indian Ocean, in 2018-2022. For each set performed by French purse seine vessels on a FAD, this dataset contains the starting and ending times allowing to have a corresponding set duration. Each time a vessel is fishing in the IBM, t_s is randomly picked from the obtained distribution of set duration. Each time a FAD is fished, a colonization time t_c is randomly picked, during which the FAD is empty. Colonization time values were generated randomly based on the daily FAD colonization rate ($1/\overline{t_c}$ with $\overline{t_c} = 40.41$ days) calculated using echosounder buoys data in the Indian Ocean by Baidai et al., 2020a.

A fourth vessel state was introduced (*idle*), to handle the vessel's behavior at low FAD numbers. When very few FADs are available, sometimes vessels do not have any occupied FAD available, i.e. $F_A^i = \varnothing$. In that case, the vessel switches to *idle* state, where it stops moving and waits for a new FAD to be available.

The detailed choice diagram used to simulate one vessel is provided in Figure 1. When several vessels target the same FAD, the first to arrive is the one performing the fishing set. If the vessels arrive at the same time-step on a FAD, the one performing the fishing set is picked randomly.

2.2 Simulations

Simulations were performed in square areas of side length L = 1,200 km, with a time-step $\Delta t = 1$ h. Fleets of V = 40 vessels were simulated during T = 360 days. To test the influence of the number of FADs and buoy information sharing on the vessels' results, several scenarios were developed. Scenarios were obtained with n ranging from 2,000 to 12,000. The values of L, V and the maximum n (12,000) were chosen to be similar to the real situation in the western Indian Ocean, were 43 purse seine vessels operate[1], with a current limit of 300 operational buoys at any one time (IOTC, 2019, 2023a), and a maximum FAD density of around 8×10^{-3} km^{-2} (Dupaix, Dagorn, et al., 2024).

We define the sharing coefficient (noted s) as the proportion of the total number of FADs from which each individual vessel receives buoy information. For each value of n, scenarios were designed with s in $\{\frac{1}{40}; \frac{1}{20}; \frac{1}{10}; \frac{1}{8}; \frac{1}{5}; \frac{1}{4}; \frac{1}{2}; 1\}$. For example, with n = 2,000 and s = 1/40, each vessel receives the information from n_f = 50 FADs. With n = 2,000 and $s = \frac{1}{10}$, vessels share their FADs by groups of 4 and hence receive information from n_f = 200 FADs. A total of 56 scenarios were simulated – one per combination of n and s values – and 100 simulations were performed for each scenario (Table 1). Each scenario considered identical vessels, traveling at the same speed (v = 19.5 km.h^{-1}, corresponding to the average speed of the cruising state in Walker and Bez, 2010), having the same detection radius (R = 12.95 km, the detection range of a bird radar, Assali et al., 2020), spending the same average time to perform a set (average t_s = 2.59 h) and having access to the information from the same number of buoys.

For each simulated vessel, we recorded the number of sets performed (N_S) and the total distance traveled (D).

[1] Query performed on https://iotc.org/oqs, 14 Feb. 2024, for year 2020, on Fishing Craft Table, of industrial purse seine vessels of EU, Seychelles and Mauritius fleets.

2.3 Profitability calculation

For each vessel in the simulations, the total distance traveled and the number of fishing sets performed were used to calculate operating costs and revenue, allowing the calculation of vessel profitability. A correction was applied to the traveled distance and the number of fishing sets to account for the fact that in the IBM, vessels are directly released in the fishing area, do not need to go back to port to unload their catch and fish for a duration of 360 days over the year. To apply this correction, we used logbook data from French purse seine vessels in the Indian Ocean, in 2019-2023. We determined the average number of days that PS vessels are active per year (noted T_a) and the proportion of each fishing trip spent traveling to the fishing zone (noted t_{travel}). The time spent traveling to the fishing zone was determined as the duration between vessel departure from port and its first fishing set plus the duration between the last fishing set and vessel arrival at port. Hence, we determined the corrected distance traveled (D') and the corrected total number of sets (N'_S) as follow:

$$D' = D \times \frac{T_a}{T}(1 - t_{travel})$$
$$N'_S = N_S \times \frac{T_a}{T}(1 - t_{travel})$$

2.3.1 Operating costs

Three costs categories were considered: (1) fuel costs, (2) FAD costs and (3) fixed and other variable costs. All the following costs provided in € were converted to USD using the 2019-2023 average conversion factor from INSEE (1 € = 1.1376 USD, French National Institute of Statistics and Economic Studies, https://www.insee.fr/fr/statistiques/2381462, accessed 2024-05-07).

Using the corrected distance travelled by vessels in the simulations, we calculated the total fuel consumption of the vessels (C, in metric tons), considering an average consumption of c = 30 kg.km^{-1} ($C = cD' \times 10^{-3}$; Basurko et al., 2022; Granado et al., 2024). Fuel costs were calculated based on C and using the average fuel cost (noted c_f, in USD.tons^{-1}) over 2019-2023, obtained from the Singapore bunker prices (https://shipandbunker.com/prices/apac/sea/sg-sin-singapore#MGO, accessed 2024-05-07). Hence, total fuel costs over the simulation period can be expressed as follow:

$$c_{fuel} = Cc_f = cD'c_f \times 10^{-3} \quad (3)$$

FAD costs included the costs associated with the buying and construction of FADs, the cost of the associated echosounder buoys and the daily cost of information transmission (subscription to the supplier). It also included the costs associated with supply vessels (SV). We estimated the FAD and echosounder buying costs to be of 1,500 € (c_{buy}). However, in the WIO, for an average of 10,700 active buoys in 2020-2023, 25,000 new buoys are activated yearly (IOTC, 2024). Hence, as we consider the number of active buoys in our simulations, a correction factor φ was applied to c_{buy} (with $\varphi = \frac{250}{107} = 2.3$, the ratio between the number of deployed buoys over a year and the average number of active buoys). The buoy information subscription cost (c_{tr}) was estimated to be 0.76 €.day^{-1} (M.Capello, pers. information), equally shared among the purse seine vessels sharing the buoy. Then, supply vessel costs were estimated using SV data provided by the Indian Ocean Tuna Commission (https://iotc.org/vessels/supply). It allowed the estimation of the average number of SV supplying each purse seine vessel between 2019 and 2023. If a SV was supplying several vessels, its cost was divided equally among the supplied purse seiners. This average number was then multiplied by a daily operational cost of 3,400 € per SV. Hence, the FAD costs can be expressed as follow:

$$c_{FADs} = \frac{\varphi n}{V}c_{buy} + T_a\frac{n_f}{sV}c_{tr} + T_a\frac{n_{SV}}{V}c_{SV} \quad (4)$$

with n the total number of FADs, V the total number of vessels, φ the ratio between the number of deployed and active buoys in the IO (IOTC, 2024), c_{buy} the individual costs of the acquisition of a FAD and the associated

buoy (USD), T_a the number of days of activity of PS vessels per year (days), n_f the number of followed FADs by the vessel, s the sharing coefficient, c_{tr} the daily cost of buoy information transmission (USD.day^{-1}), n_{SV} the total number of SV (from IOTC data) and c_{SV} the daily operational cost of a SV (USD.day^{-1}).
Finally, fixed and other variable costs (c_{fixed}) were estimated to be of 17,000 € per day. These costs include vessel and material reparation, fishermen' salary and transportation to the Indian Ocean.

2.3.2 Revenue

Revenue were calculated estimating catch of the three main commercial categories of tropical tuna (Guillotreau et al., 2024): large yellowfin > 10 kg (noted YFT), skipjack tuna of all size (SKJ) and mixed tunas which are a mixture of albacore, frigate tuna, bigeye tuna and juvenile yellowfin tunas < 10 kg (MIX). Compared to categories used in Guillotreau et al., 2024, frigate tuna was added to the MIX category as the amount of catch of this species by PS strongly increased since 2018 (average yearly catch of 1,940 metric tons in 2019-2022, IOTC data).
Logbook data from French purse seine vessels in the Indian Ocean, from 2019-2023, was used to calculate the average catch-per-set of each of the above categories. In order to improve the accuracy of the estimated catches, FOB-associated catch-per-set reported in vessel logbooks was corrected using a dedicated procedure referred to as levels 1 and 2 of the T3 processing (Duparc et al., 2020). Level 1 adjusts the catch-per-set values declared in vessel logbooks using landing notes, to improve the accuracy of catch estimates provided by skippers. Level 2 estimates the species and size compositions of FOB sets based on port sampling data. Similarly to aCAT and aCRT values (see Section 2.1.1), catch-per-set values were corrected using the model of tuna behavior adapted from Capello et al., 2022 (Figure S1). The total amout of YFT and BET of all size caught in the simulations was recorded, to compare it with corresponding quotas in the IO (quota for the EU, MUS and SYC fleets: 113,432 t YFT, IOTC Res 21/01 and 20,861 t BET, IOTC Res 23/04).
Average sale prices of the three categories (SKJ, YFT and MIX) over 2019-2023 were extracted from tuna sale prices in Bangkok market (http://www.customs.go.th/statistic_report.php, SKJ HS-Code: 03034300000, YFT HS-Code: 03034200000, accessed 2024-04-29). The sale price of MIX was estimated to be equal to the SKJ sale price. The revenue for each vessel can be expressed as follow:

$$r = \left(p_{yft} YFT + p_{skj} SKJ + p_{mix} MIX\right) N'_s \tag{5}$$

where p_{yft}, p_{skj} and p_{mix} are the sale prices of yellowfin, skipjack and mixed tuna respectively (in USD.t^{-1}), YFT, SKJ and MIX the average catch-per-set of yellowfin, skipjack and mixed tuna (in tons) and N'_s the corrected number of sets performed by the simulated PS vessel over a year.

2.3.3 Profitability

The profitability (π, in USD) of each vessel was calculated as follows, using costs and revenue estimations from Eq. 3,4 and 5:

$$\pi = r - T_a c_{fixed} - c_{fuel} - c_{FADs} \tag{6}$$

Based on the revenue calculated for each vessel, Gini indices (G) were calculated for each simulation, based on the following equation:

$$G = \frac{1}{\overline{r}} \frac{1}{V^2} \sum_{i=1}^{V} \sum_{j=1}^{V} |r_i - r_j| \tag{7}$$

where $\overline{r}$ is the average vessel revenue in the simulation, r_i is the revenue of vessel i and V is the number of vessels ($V = 40$). Here, the Gini index is an index of revenue dispersion among vessels. $G = 0$ would represent perfectly distributed revenue, when $G = 1$ would mean that one vessel gets all the generated revenue.

2.4 Social costs

2.4.1 Silky shark bycatch

Because no aCAT nor aCRT are available for silky sharks, we considered every fished FAD to be occupied by an average number of SLK (m_{SLK}). The calculation of this average value is detailed in Supplementary S1. Based on this average number of silky shark caught per set, the total amount of bycatch was then determined for every scenario.

Purse seine vessels discard bycaught silky sharks, so to quantify the induced economic damage one needs to account for the commercial, recreational and conservation values of sharks (M Tolotti et al., 2022). Based on M Tolotti et al., 2022's work, the cost of catching an individual SLK was quantified as the forgone consumptive value of sharks. This value included the value of shark fins and that of fresh meat, corresponding to a cost of 3.98 USD per kg of bycaught SLK. Bycaight sharks were considered to weight an average of 12.1 kg per individual (M Tolotti et al., 2022).

2.4.2 FAD stranding

To determine the external costs associated with FAD stranding, we first determined the number of FADs per vessel expected to strand for every scenario. For a vessel i this number (noted $n_{STR}(i)$) can be expressed as follows:

$$n_{STR}(i) = \frac{\varphi n}{V} p_{STR} \tag{8}$$

where n is the total number of active buoys, V the number of vessels ($V = 40$) and φ is the ratio between the number of deployed buoys over a year and the average number of active buoys ($\varphi = \frac{250}{107} = 2.3$, Section 2.3) (IOTC, 2024). p_{STR} is the proportion of deployed FADs that end up stranding. This proportion was estimated at 17.5 % of the number of deployed FADs in the Indian Ocean, using only active buoys (Imzilen, Lett, Chassot, and Kaplan, 2021). Later, using data from deactivated buoys in the Indian Ocean, it was determined that this percentage was underestimated by 23.7 % (Lau-Medrano, Gaertner, Marsac, Guéry, et al., 2024). Hence, we use $p_{STR} = 0.175 \times 1.237 = 0.216$, *i.e.* 21.6 % of deployed FADs strand.

A literature review was then performed to assess the average FAD weight when recovered on a beach and the costs associated with beach clean-ups (Table 2). Few articles estimated the wet weight of FADs when recovered and both estimations were above 1 ton. Costs associated with beach clean-ups varied from 323 to 29,104 USD per ton of litter. In the analysis, we considered a conservative estimation of FAD stranding external costs, considering an average wet-weight of 1.22 tons per FAD (Burt et al., 2020) and a clean-up cost of 1,138 USD per ton of litter (Cruz et al., 2020).

3 Results

3.1 Simulation outputs

The average simulated number of sets per day ranged between 0.45 and 2.69 depending on the scenario, with a median value of 0.87 (Figure 2A). This corresponded to an average catch per day ranging between 13.3 and 79.5 t of tuna, with a median value of 27 metric tons. The average number of sets per day reached its maximum value for the scenario with maximum values of n and s. When n = 2,000, the number of sets per day first decreased with increasing s values, then increased again, above s = 0.1. When $n \geq$ 3,000, the number of sets per day displayed an increasing trend with increasing values of s. Traveled distance per day ranged between 84 km and 397 km, corresponding to a total fuel consumption over a year of 666 t and 3,152 t respectively. The fuel consumption displayed inverted trends compared to the number of sets per day (Figure 2B). Vessels spent time in *idle* state in six scenarios (n = 2,000 and $s \in \{0.025, 0.05, 0.1, 0.125\}$ and n = 3,000 and $s \in \{0.025, 0.05\}$) but this time only reached a maximum of 2.1 % when n = 2,000 and s = 0.025. This

result suggest that the number of available FADs was a limitation only in scenarios with small n and s values (Figure 2C). Fishing vessels fished mainly on followed FADs, for all scenarios, with the percentage of fishing sets performed on non-followed FADs varying between 0 and 16.1 %. This percentage was highest for small s values and decreased with the increase of n (Figure 2D).

3.2 Profitability and equity among vessels

Average profitability per scenario varied between -3.4 and 25.9 million USD per vessel, with positive average π attained in most scenarios (47 out of 56 scenarios, Figure 3). The highest profitability was reached for highest n and s values, while the lowest was reached for highest n and lowest s values. At a fixed value of n, except when n = 2,000, increasing the sharing coefficient increased the average profitability of the vessels. In the scenarios with π values above 6.9 million USD, the total amount of BET caught or both the amount of YFT and BET exceeded the quotas existing in the Indian Ocean, setting an upper limit to the increase of π.

Average Gini index (G) varied between 9.05×10^{-3} and 1.09×10^{-1} (Figure 4). For fixed values of n, when $n \leq$ 3,000, increasing information sharing increased revenue inequity and the variability of G between simulations (Figure 4). However, when $n \geq$ 4,000, increasing information sharing induced a decreasing trend of G *-i.e.* a increase in equity among vessels. This result implies that, when the total number of active buoys present in the system is low, increasing the sharing of buoy information will increase the competition between vessels and therefore the inequality. However, this is true only when the number of active buoys is strictly below 4,000, so at a point much lower than the current situation in the Western Indian Ocean.

3.3 Private and social costs

A smaller number of FADs with a larger spread of information reduced the costs associated with FAD fishing, when considering all the costs together (Figure 5). Diminishing the total number of active buoys n lowered both private costs (fuel and FAD operating costs) and social costs associated with FAD stranding. Sharing buoy communications on a larger scale allowed to reduce fuel costs but did not influence FAD stranding nor FAD operating costs. Fuel costs varied between 0.5 and 2.2 USD million per vessel, the minimum value being found for n = 12,000 and s = 1 and the maximum for n = 12,000 and s = 0.025. FAD costs varied between 1.3 USDM (n = 12,000) and 0.2 USDM (n = 2,000). Stranding costs were the highest costs (average value of 4.8 USDM across all scenarios) but they sharply decreased if the total number of active buoys fell, from 9.0 USDM (n = 12,000) to 1.5 USDM (n = 2,000). Depending on the scenario, silky shark bycatch varied between 0.45 and 1.95 tons per year per vessel. For a fixed total number of active buoys, it increased with shared information. When the sharing rate was low ($s \leq 0.1$), reducing the number of FADs n amplified SLK bycatch. If $s > 0.1$, the relationship between SLK bycatch and n was non-linear, bycatch being maximal for intermediate n values (between 3,000 and 6,000). Social costs associated with silky shark bycatch were deemed low, varying between 0.04 USDM and 0.31 USDM. However, they were the only costs that increased with shared knowledge.

4 Discussion

Purse seine (PS) fleets in the Indian Ocean are a canonical example of a highly efficient fleet facing catch limits and which presents endogenous overcapacity (Tidd, Dagorn, et al., 2025). Technical change, specifically the introduction of echosounder buoys in the early 2010s, enhanced dramatically the fishing efficiency of PS fleets (Tidd, Floc'h, et al., 2023; Wain et al., 2021). This higher efficiency, combined with the absence of quotas on tropical tunas until 2017 resulted in a 'race to fish', and a substantial overcapacity of the fleet. For example, the tonnage of fish caught by French purse seiners in the IO could be captured with 21 % less vessels utilized at their full capacity (Tidd, Dagorn, et al., 2025). The current regulation addressing this problem lies in the adoption of catch limits, since 2017 and 2024 for yellowfin (YFT) and bigeye (BET) tuna respectively. Catch limits may prove efficient to manage target species populations (Hoshino et al., 2020), and even to reduce

some negative externalities of fishing – *e.g.* a reduction of fishing effort can also lead to a reduction of carbon emissions (Waldo et al., 2016). But many ecological impacts are not accounted for by such simple measures and single-species management often results in new types of negative externalities (Martinet and Blanchard, 2009; M Tolotti et al., 2022).

Through the development of an Individual-Based Model, we demonstrate that knowledge sharing can allow the reduction of FAD numbers, reducing several impacts of FADs without reducing PS fleets' economic profitability. First, due to the current state of overcapacity, reducing the total number of FADs would enhance individual vessels' profitability by lowering costs without impacting revenues, while addressing additional externality issues (lower carbon emissions due to shorter traveled distance and avoidance of FAD stranding). An optimum number of FADs can be found with a reduction by a factor 4 although a further step in the reduction process would intensify competition between vessels. A shared access to satellite buoy communications would not only contribute to save search costs (*e.g.* the use of supply vessels) for private benefits, they would also reduce the social costs of air and water pollution (CO2, SO2 and NOx emissions, FAD sinking or stranding, degradation of marine habitats, etc) to a significant extent. By upgrading the efficiency of the fleet, moving towards a fully shared knowledge between vessels is likely to exceed YFT and BET quotas allocated to PS fleets in the IO, amplifying the current overcapacity problem. Consequently, such a shift should be complemented by a limitation of the fishing effort or of the fleet capacity (Tidd, Dagorn, et al., 2025).

The models developed in this study rely on a number of simplifications that may influence the obtained results. First, the model used to determine tuna and silky shark dynamics at FADs (adapted from the NS scenario in Capello et al., 2022) does not account for the social behavior of these species. Capello et al., 2022 developed several social scenarios in their model and demonstrated that social behavior influences the way the fraction of schools which are associated varies with FAD density. Hence, we could expect the implementation of tuna and silky shark social behavior in our modeling framework to impact the obtained results. However, a sensitivity analysis, using no behavioral model instead of the non-social model presented here showed very similar results, suggesting that the impact of the marine species behavioral model is limited. Secondly, the behavior of the PS vessels operating in our model was simplified, with vessels always targeting the closest occupied FAD, and staying in $idle$ state when no FAD was available. Also, we did not account for free-swimming school fishing, as simulated vessels only fished on associated schools. These simplifications could bring uncertainty on the obtained results. However, scenarios close to the current situation in the IO (n = 12,000 and s between 0.1 and 0.2) resulted in an average of 0.8 to 1.1 set per day, corresponding to 24 to 33 tons of tuna caught daily, consistent with observed values (Lau-Medrano, Gaertner, Marsac, and Kaplan, 2025). Moreover, vessels switched to $idle$ state in very few scenarios and for a very small proportion of the simulated time (maximum of 2.1 % in one scenario). These elements support the reliability of our results.

Given the current dynamics of entry and exit within the Indian Ocean PS fleet – marked by an increase in vessel numbers among countries that opposed resolutions introducing catch limits (IOTC, 2021, 2023b) – the practical implementation of knowledge-sharing mechanisms may prove challenging. A first approach could strive to minimize coordination costs through an integrated organizational structure. Several pathways can be envisioned. One option involves the establishment of a centralized entity responsible for managing FADs at the ocean-wide level. This organization could be jointly financed by fishing companies and administered either by a coalition of industry actors or directly by the Regional Fisheries Management Organization itself. Such a joint-venture or eco-organization could also provide a FAD recovery service, aimed at mitigating water pollution and coral reef degradation caused by abandoned gears (Imzilen, Lett, Chassot, and Kaplan, 2021).

Alternatively, fostering individual incentives for information sharing may encourage behavior aligned with conservation objectives (Hilborn et al., 2005). For example, fishers could be granted preferential access to quotas, reduced monitoring requirements, or eligibility for eco-certification schemes that enhance market value in exchange for knowledge sharing. These incentives could be combined with an effort to go towards

participatory management. Participatory management which includes stakeholders in the decision process has been shown to be essential for sustainable resource management (Kapoor, 2001; Quimby and Levine, 2018), as it increases environmental learning (Fujitani et al., 2017), can allow to combine traditional ecological knowledge with conventional science (Bay et al., 2023) and, increases stakeholders trust, acceptance of and compliance with regulations (Alpízar, 2006; Delaney et al., 2023; Holm and Soma, 2016).

5 Acknowledgements

We thank IRD's Ob7 ("Observatoire des Ecosystèmes Pélagiques Tropicaux Exploités") in charge of French logbook data collection, processing, management, and for sharing the data used in this study. We also thank the BAEI (Bureau des Affaires Européennes et Internationnales) from the French DGAMPA (Direction Générale des Affaires Maritimes, de la Pêche et de l'Aquaculture) for their help on the current regulation and quotas applying to PS fishing vessels in the Indian Ocean, IOTC Secretariat for the instrumented buoys data collection, processing and management, and ISSF for partial financial support and its involvement in the overall project. This work was supported by the MANFAD project (France Filière Pêche), URL: https://manfad-project.com.

6 Conflict of interest disclosure

The authors declare having no financial conflicts of interest in relation to the content of the article.

7 Figures

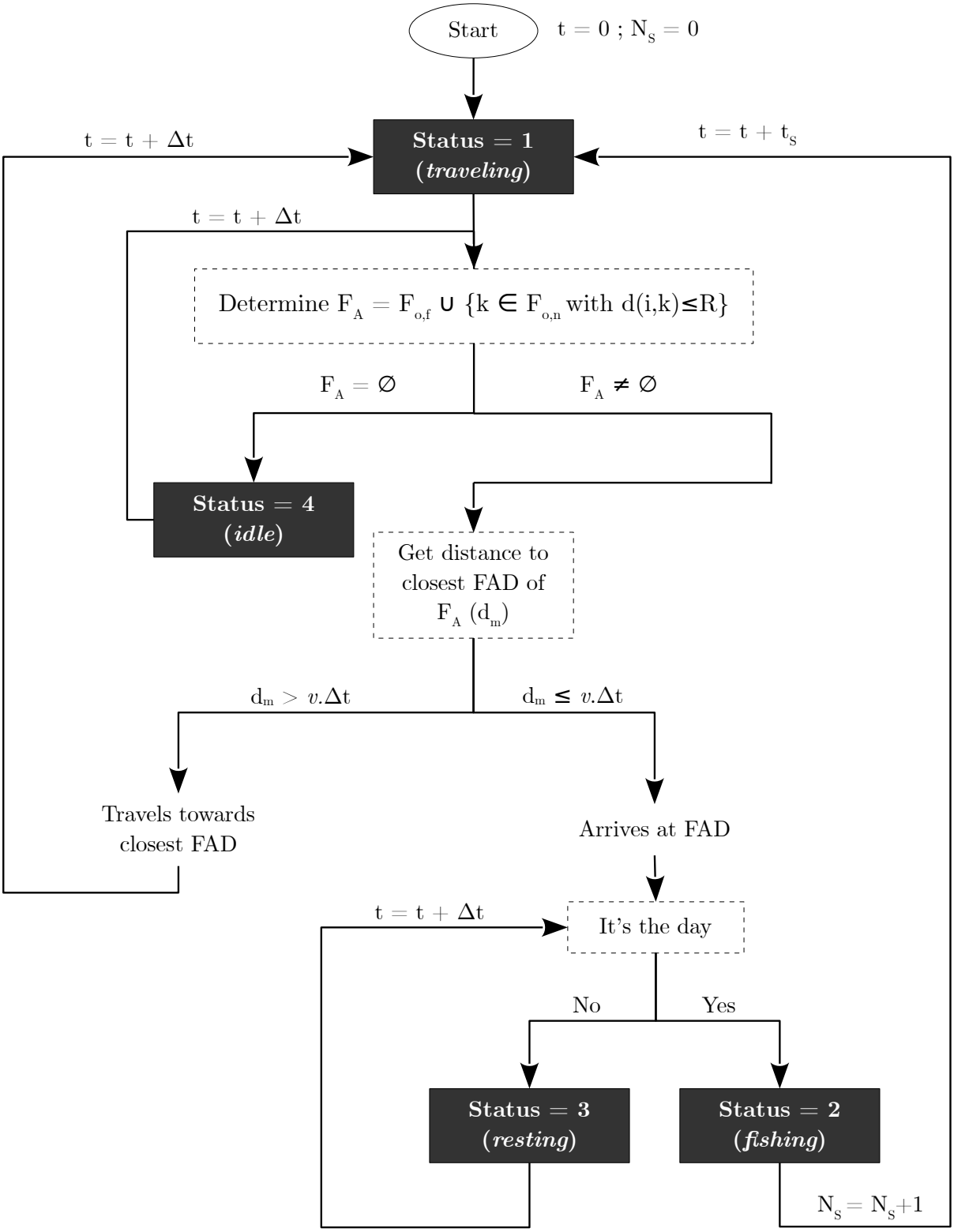

Figure 1. Choice diagram of the Individual-Based Model, applied to vessel *i*. t is the current time in the simulation, N_S the number of performed fishing sets, Δt the time-step duration, F_A the set of all the FADs available to be fished by vessel i (see Eq 2), d_m the distance between vessel i and the aim FAD, v the vessel speed.

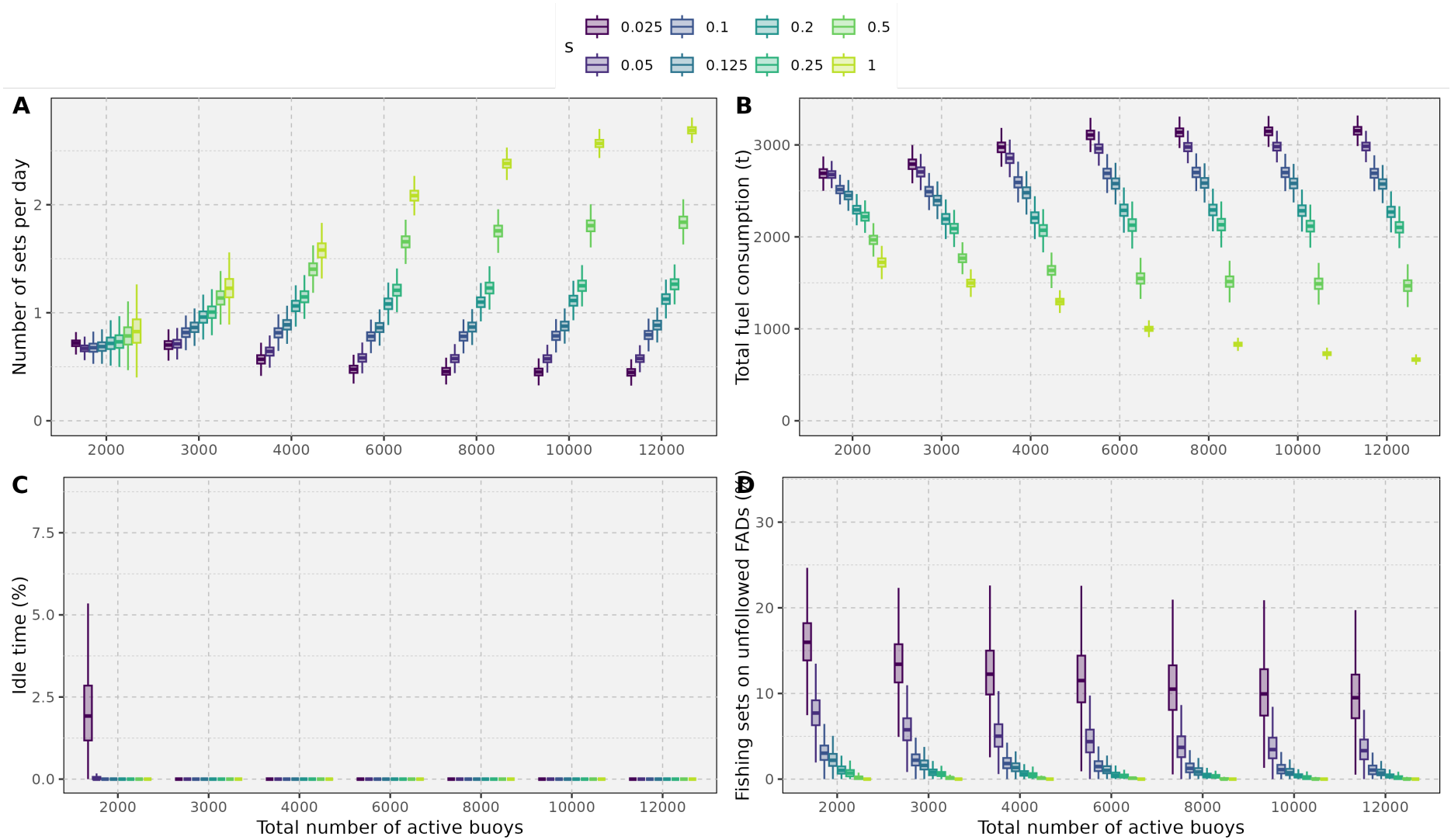

Figure 2. Boxplots of the main simulations outputs. (A) Number of fishing sets performed by purse seine vessels per day. **(B)** Fuel consumption (in metric tons) per purse seine vessels over the whole simulation period. **(C)** Percentage of idle time over the whole simulation duration. **(D)** Percentage of the fishing sets performed on unfollowed FADs, i.e randomly encountered FADs. Colors correspond to the sharing coefficient (s), i.e. the proportion of the total number of buoys each vessel has access to.

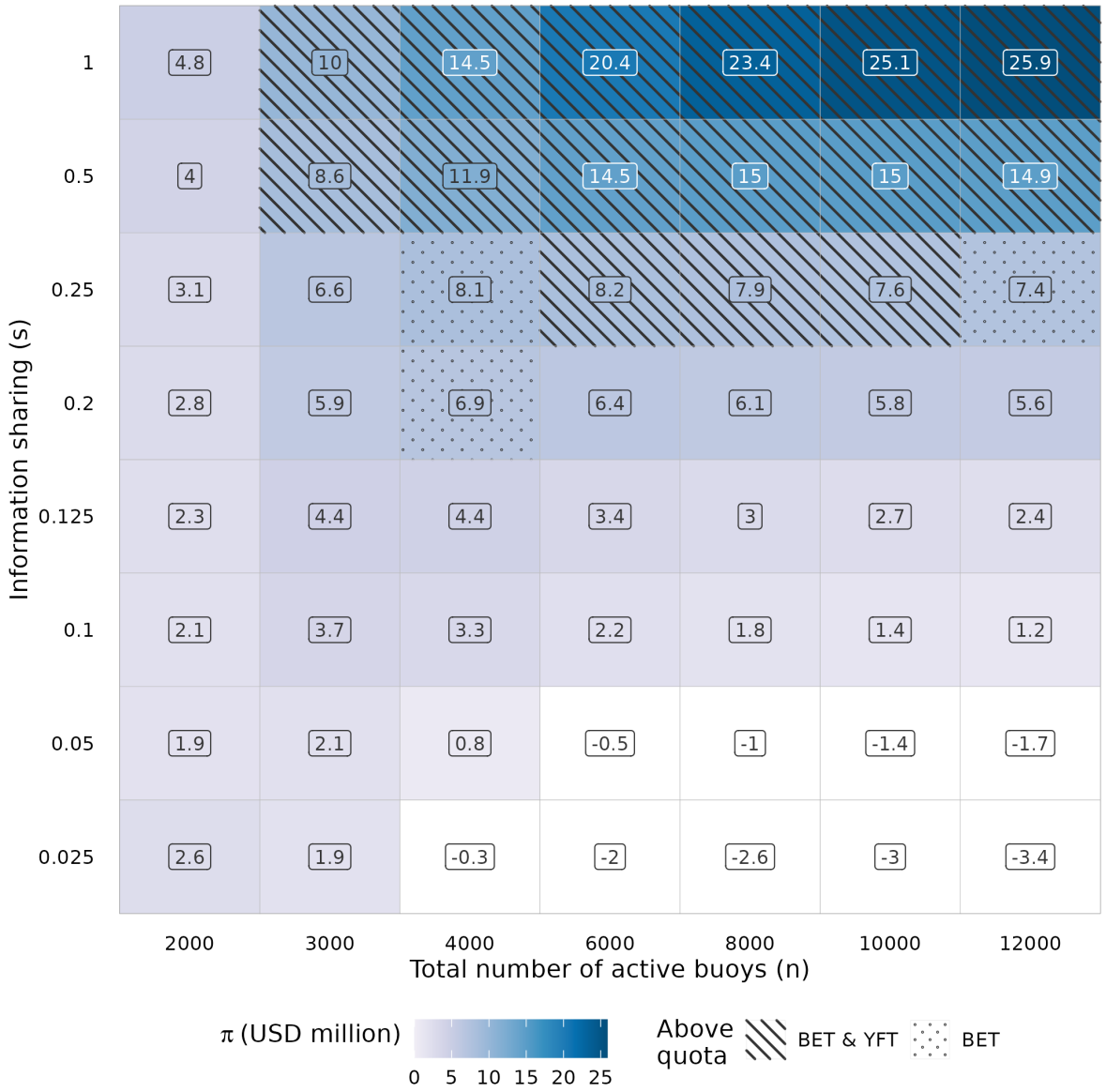

Figure 3. Average profitability π of simulated purse seine vessels for every scenario. Above Indian Ocean quotas: cells are dotted when the total catch is above the BET quota, and hatched when the total catch is above both the YFT and the BET.

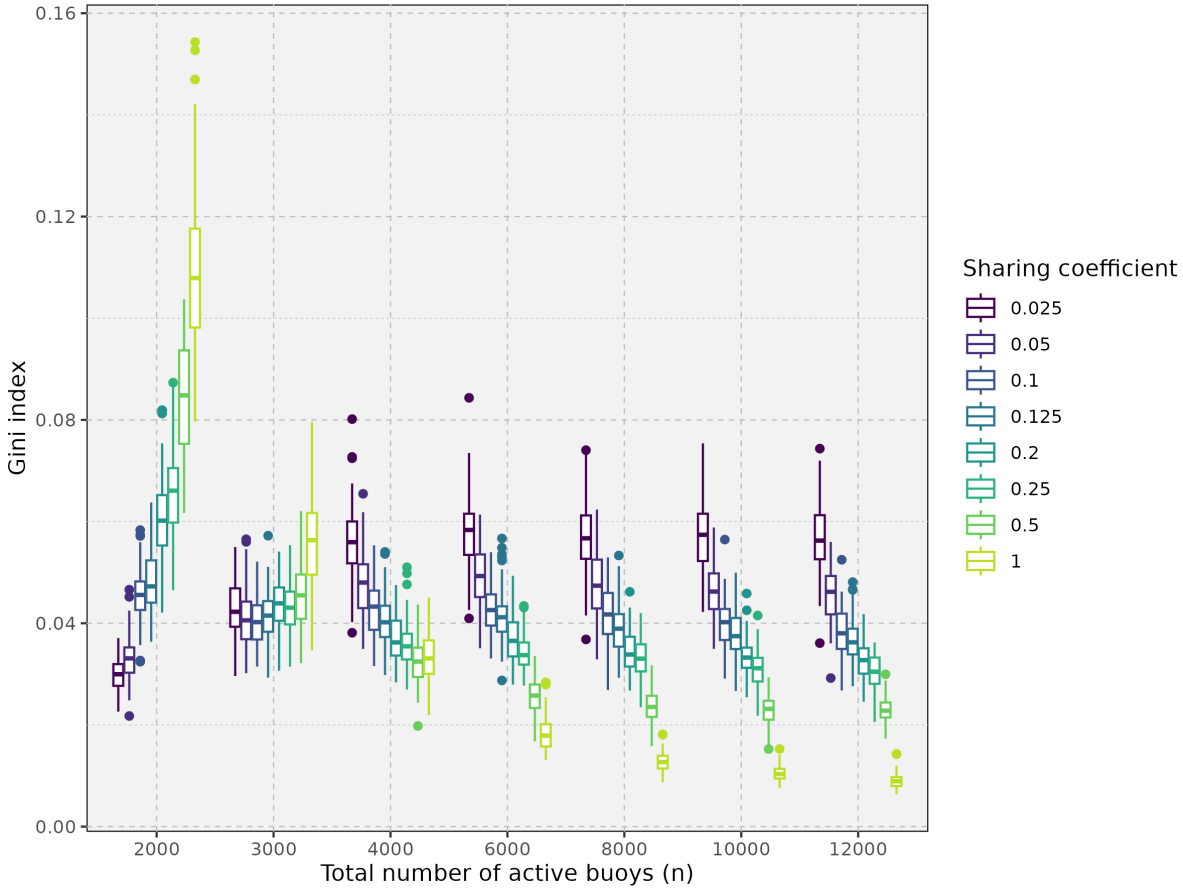

Figure 4. Boxplot of the Gini index calculated on the vessels' revenue per scenario.

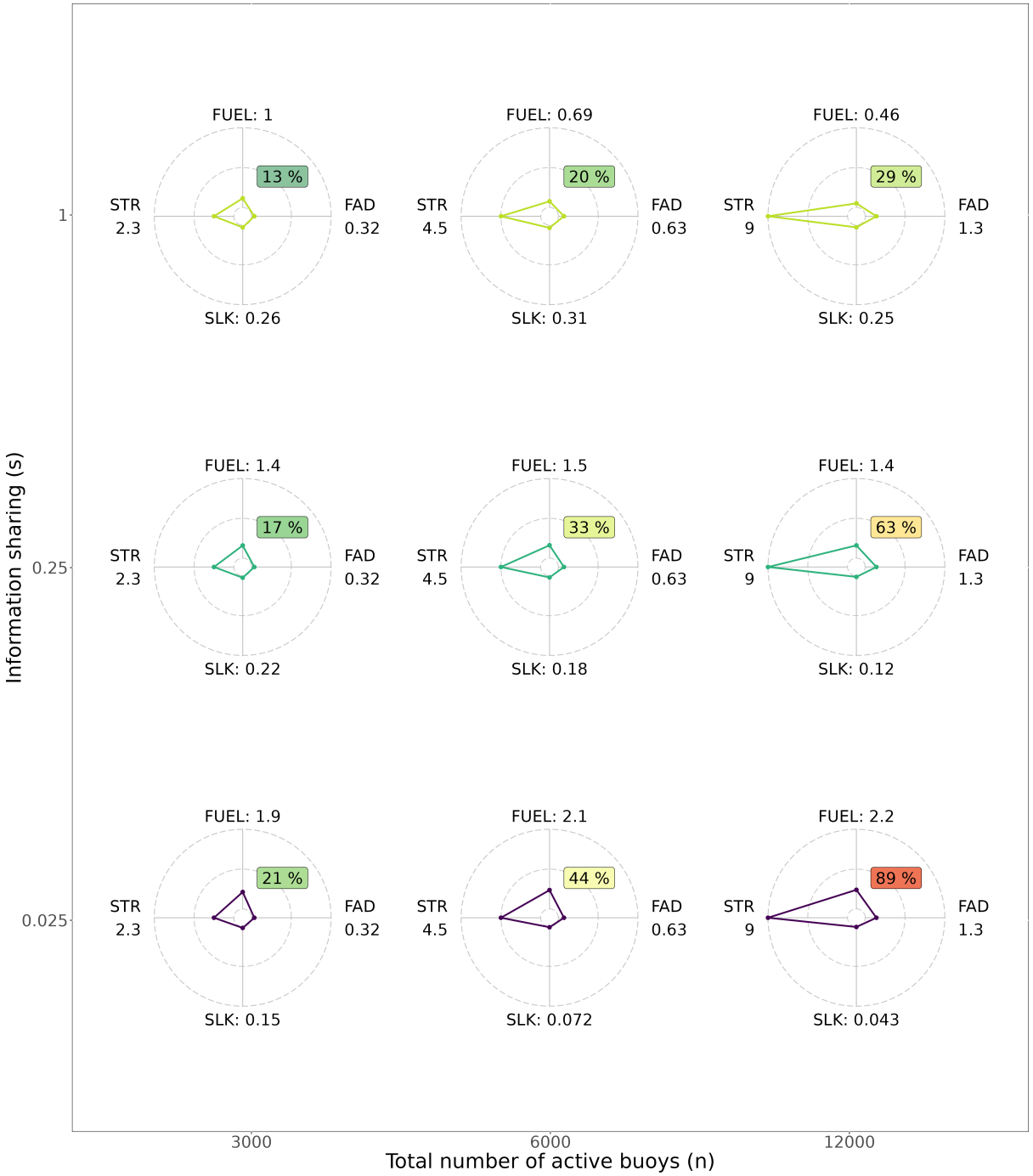

Figure 5. Private and social costs associated with FAD fishing. Radar charts of costs for several scenarios. Social costs include costs from stranded FAD's cleaning (STR) and costs induced by silky shark bycatch (SLK). Private costs include fuel costs (FUEL) and FAD structural costs (buying + information + supply costs, FAD). All costs are indicated in USD millions. Percentages on each radar chart indicate the area of the polygon divided by the area of the biggest possible polygon. n is the total number of active buoys and s the sharing coefficient.

8 Tables

Table 1. Summary of the performed scenarios. Each scenario was simulated 100 times. n: total number of followed buoys, s: buoy sharing coefficient, V total number of vessels, Δt: time-step, T: total simulation duration, L: side length of the simulation square, v: vessel speed, R: detection radius.

Parameters	Values
Varying parameters	
n	2,000; 3,000; 4,000; 6,000; 8,000; 10,000; 12,000
s	1/40, 1/20, 1/10, 1/8, 1/5, 1/4, 1/2, 1
Fixed parameters	
V	40 vessels
Δt	1 hour
T	360 days
L	1,200 km
v	19.5 km.h^{-1}
R	12.95 km

Table 2. Estimations of beach clean-up individual costs and FAD wet weight from the literature.

Value	Unit	Year	Location	Reference
29,104	USD per ton of litter	2021	South Africa	Jain et al., 2021
1,784	USD per ton of litter	2022	Grenada	Raes et al., 2022b
323	USD per ton of litter	2022	Saint Lucia	Raes et al., 2022a
3,678	USD per ton of litter	2022	Antigua and Barbuda	Mittempergher et al., 2022
8,737	USD per ton of litter	2020	Seychelles	Burt et al., 2020
7,354 to 22,063[a]	USD per ton of litter	2017	Indonesia	Lindstrand and Thunell, 2017
1,138	USD per ton of litter	2020	Spain	Cruz et al., 2020
721	USD per ton of litter	2010	South Korea	Han et al., 2010
1,322	USD per ton of litter	2021	Spain	Sanabria Garcia and Raes, 2021
1.22	FAD wet weight in tons	2020	Seychelles	Burt et al., 2020
1.5	FAD wet weight in tons	2021	WCPO	Purves et al., 2021

[a] Depending on the daily salary considered (from 47 to 142 euros)

References

Alpízar MAQ (Nov. 2006). Participation and fisheries management in Costa Rica: From theory to practice. *Marine Policy* 30, 641–650. ISSN: 0308-597X. https://doi.org/10.1016/j.marpol.2005.09.001.

Ariz J, A Delgado, A Fonteneau, F Gonzalez Costas, and P Pallares (1999). Logs and tunas in the Eastern Tropical Atlantic. A review of present knowledge and uncertainties. In: *Proceedings of the International Workshop on Fishing for Tunas Associated with Floating Objects*. Ed. by Scott MD, Bayliff WH, Lennert-Cody CE, and Schaefer KM. Vol. 11. La Jolla, CA, February 11-13, 1992: Inter-American Tropical Tuna Commission, pp. 21–65.

Assali C, N Bez, and Y Tremblay (2020). Raking the ocean surface: new patterns of coordinated motion in seabirds. en. *Journal of Avian Biology* 51. _eprint: https://onlinelibrary.wiley.com/doi/pdf/10.1111/jav.02258. ISSN: 1600-048X. https://doi.org/10.1111/jav.02258.

Baidai Y, L Dagorn, MJ Amande, D Gaertner, and M Capello (2020a). Tuna aggregation dynamics at Drifting Fish Aggregating Devices: A view through the eyes of commercial echosounder buoys. *ICES Journal of Marine Science* 77, 2960–2970. https://doi.org/10.1093/icesjms/fsaa178.

Baidai Y, L Dagorn, MJ Amande, D Gaertner, and M Capello (2020b). Machine learning for characterizing tropical tuna aggregations under Drifting Fish Aggregating Devices (DFADs) from commercial echosounder buoys data. *Fisheries Research* 229, 105613. https://doi.org/10.1016/j.fishres.2020.105613.

Basurko OC, G Gabiña, J Lopez, I Granado, H Murua, JA Fernandes, I Krug, J Ruiz, and Z Uriondo (Jan. 2022). Fuel consumption of free-swimming school versus FAD strategies in tropical tuna purse seine fishing. en. *Fisheries Research* 245, 106139. ISSN: 0165-7836. https://doi.org/10.1016/j.fishres.2021.106139.

Bay LK, J Gilmour, B Muir, and PE Hardisty (Aug. 2023). Management approaches to conserve Australia's marine ecosystem under climate change. *Science* 381. Publisher: American Association for the Advancement of Science, 631–636. https://doi.org/10.1126/science.adi3023.

Burt AJ, J Raguain, C Sanchez, J Brice, F Fleischer-Dogley, R Goldberg, S Talma, M Syposz, J Mahony, J Letori, C Quanz, S Ramkalawan, C Francourt, I Capricieuse, A Antao, K Belle, T Zillhardt, J Moumou, M Roseline, J Bonne, R Marie, E Constance, J Suleman, and LA Turnbull (Sept. 2020). The costs of removing the unsanctioned import of marine plastic litter to small island states. en. *Scientific Reports* 10. Publisher: Nature Publishing Group, 14458. ISSN: 2045-2322. https://doi.org/10.1038/s41598-020-71444-6.

Capello M, J Rault, JL Deneubourg, and L Dagorn (Aug. 2022). Schooling in habitats with aggregative sites: The case of tropical tuna and floating objects. en. *Journal of Theoretical Biology* 547, 111163. ISSN: 0022-5193. https://doi.org/10.1016/j.jtbi.2022.111163.

Cruz CJ, JJ Muñoz-Perez, MI Carrasco-Braganza, P Poullet, P Lopez-Garcia, A Contreras, and R Silva (Apr. 2020). Beach cleaning costs. *Ocean & Coastal Management* 188, 105118. ISSN: 0964-5691. https://doi.org/10.1016/j.ocecoaman.2020.105118.

Dagorn L, N Bez, T Fauvel, and E Walker (May 2013). How much do fish aggregating devices (FADs) modify the floating object environment in the ocean? en. *Fisheries Oceanography* 22. L, 147–153. ISSN: 10546006. https://doi.org/10.1111/fog.12014.

Delaney A, DG Reid, C Zimmermann, M Kraan, NA Steins, and MJ Kaiser (Apr. 2023). Socio-Technical Approaches are Needed for Innovation in Fisheries. *Reviews in Fisheries Science & Aquaculture* 31. Publisher: Taylor & Francis _eprint: https://doi.org/10.1080/23308249.2022.2047886, 161–179. ISSN: 2330-8249. https://doi.org/10.1080/23308249.2022.2047886.

Dupaix A (2023). Impacts des modifications de l'habitat pélagique sur le comportement et la condition physiologique des thons tropicaux. en. PhD. Sète, France: Université de Montpellier.

Dupaix A, M Capello, C Lett, M Andrello, N Barrier, G Viennois, and L Dagorn (Sept. 2021). Surface habitat modification through industrial tuna fishery practices. *ICES Journal of Marine Science* 78, 3075–3088. ISSN: 1054-3139. https://doi.org/10.1093/icesjms/fsab175.

Dupaix A, L Dagorn, JL Deneubourg, and M Capello (Sept. 2024). Quantifying the impact of habitat modifications on species behavior and mortality: The case-study of tropical tuna. *Ecological Applications* 34, e3018. https://doi.org/10.1002/eap.3018.

Dupaix A, F Ménard, JD Filmalter, Y Baidai, N Bodin, M Capello, E Chassot, H Demarcq, JL Deneubourg, A Fonteneau, F Forget, F Forrestal, D Gaertner, M Hall, KN Holland, D Itano, DM Kaplan, J Lopez, F Marsac, A Maufroy, G Moreno, JA Muir, H Murua, L Roa-Pascuali, G Pérez, V Restrepo, M Robert, KM Schaefer, G Sempo, M Soria, and L Dagorn (May 2024). The challenge of assessing the effects of drifting fish aggregating devices on the behaviour and biology of tropical tuna. *Fish and Fisheries* 25, 381–400. https://doi.org/10.1111/faf.12813.

Duparc A, M Depetris, L Floch, P Cauquil, P Bach, and J Lebranchu (2020). *Development status of the new tropical tunas treatment (t3) software*. Tech. rep. IOTC-2020-WPTT22(DP)-INF01. Indian Ocean Tuna Commission.

Escalle L, J Mourot, T Thellier, J Lopez, LM Fuller, J Wichman, S Royer, L Hood, B Bigler, B Jaugeon, T Nicholas, K Pollock, F Prioul, A Marks, M Kutan, J Jones, J Lynch, H Tait, and P Hamer (2023). *Analyses of the regional database of stranded (dFAD) in the EPO*. en. 7th ad-hoc permanent working group on FADs FAD-07-INF-A. La Jolla, CA: Inter-American Tropical Tuna Commission.

Escalle L, JS Phillips, M Brownjohn, S Brouwer, AS Gupta, EV Sebille, J Hampton, and G Pilling (Sept. 2019). Environmental versus operational drivers of drifting FAD beaching in the Western and Central Pacific Ocean. en. *Scientific Reports* 9. L, 1–12. ISSN: 2045-2322. https://doi.org/10.1038/s41598-019-50364-0.

Filmalter JD, M Capello, JL Deneubourg, PD Cowley, and L Dagorn (Aug. 2013). Looking behind the curtain: quantifying massive shark mortality in fish aggregating devices. en. *Frontiers in Ecology and the Environment* 11. L, 291–296. ISSN: 1540-9295. https://doi.org/10.1890/130045.

Fonteneau A, E Chassot, and D Gaertner (2015). Managing tropical tuna purse seine fisheries through limiting the number of drifting fish aggregating devices in the Atlantic: food for thought. en. *Collect. Vol. Sci. Pap. ICCAT* 71. NL, 460–475.

Fujitani M, A McFall, C Randler, and R Arlinghaus (June 2017). Participatory adaptive management leads to environmental learning outcomes extending beyond the sphere of science. *Science Advances* 3. Publisher: American Association for the Advancement of Science, e1602516. https://doi.org/10.1126/sciadv.1602516.

Gershman D, A Nickson, and M O'Toole (2015). *Estimating the Use of FADs Around the World*. Tech. rep. L. PEW Charitable Trusts.

Gilman EL (Sept. 2011). Bycatch governance and best practice mitigation technology in global tuna fisheries. en. *Marine Policy* 35, 590–609. ISSN: 0308-597X. https://doi.org/10.1016/j.marpol.2011.01.021.

Govinden R, M Capello, F Forget, JD Filmalter, and L Dagorn (Mar. 2021). Behavior of skipjack (*Katsuwonus pelamis*), yellowfin (*Thunnus albacares*), and bigeye (*T. obsesus*) tunas associated with drifting fish aggregating devices (dFADs) in the Indian Ocean, assessed through acoustic telemetry. en. *Fisheries Oceanography* 30. _eprint: https://onlinelibrary.wiley.com/doi/pdf/10.1111/fog.12536, 542–555. ISSN: 1365-2419. https://doi.org/10.1111/fog.12536.

Granado I, L Hernando, Z Uriondo, and JA Fernandes-Salvador (Jan. 2024). A fishing route optimization decision support system: The case of the tuna purse seiner. *European Journal of Operational Research* 312, 718–732. ISSN: 0377-2217. https://doi.org/10.1016/j.ejor.2023.07.009.

Guillotreau P, F Salladarré, M Capello, A Dupaix, L Floc'h, A Tidd, M Tolotti, and L Dagorn (Jan. 2024). Is FAD fishing an economic trap? Effects of seasonal closures and other management measures on a purse-seine tuna fleet. *Fish and Fisheries* 25, 151–167. https://doi.org/10.1111/faf.12799.

Hall M (1992). The association of tunas with floating objects and dolphins in the Eastern Pacific Ocean. 1992. Part VII. Some hypotheses on the mechanisms governing the association of tunas with floating objects and dolphins. In: *International Workshop on Fishing for Tunas Associated with Floating Objects*. Ed. by Scott MD, Bayliff WH, Lennert-Cody CE, and Schaefer KM. La Jolla, CA, February 11-13, 1992: Inter-American Tropical Tuna Commission.

Hallier JP and J Parajua (1999). Review of tuna fisheries on floating objects in the Indian Ocean. In: *Proceedings of the International Workshop on Fishing for Tunas Associated with Floating Objects*. Ed. by Scott MD, Bayliff

WH, Lennert-Cody CE, and Schaefer KM. Vol. 11. La Jolla, CA, February 11-13, 1992: Inter-American Tropical Tuna Commission, pp. 195–221.

Han S, H Kim, S Kim, and H Noh (2010). South Korea coastal cleanup program for marine litter. In: *C. Morishige (Ed.), Marine debris prevention projects and activities in the Republic of Korea and United States: A compilation of project summary reports*. National Oceanic Atmospheric Administration, pp. 9–15.

Hilborn R, JM(Orensanz, and AM Parma (Jan. 2005). Institutions, incentives and the future of fisheries. *Philosophical Transactions of the Royal Society B: Biological Sciences* 360. Publisher: Royal Society, 47–57. https://doi.org/10.1098/rstb.2004.1569.

Holm P and K Soma (Feb. 2016). Fishers' information in governance — a matter of trust. *Current Opinion in Environmental Sustainability*. Sustainability governance and transformation 2016: Informational governance and environmental sustainability 18, 115–121. ISSN: 1877-3435. https://doi.org/10.1016/j.cosust.2015.12.005.

Hoshino E, I van Putten, S Pascoe, and S Vieira (Mar. 2020). Individual transferable quotas in achieving multiple objectives of fisheries management. *Marine Policy* 113, 103744. ISSN: 0308-597X. https://doi.org/10.1016/j.marpol.2019.103744.

Imzilen T, C Lett, E Chassot, and DM Kaplan (Feb. 2021). Spatial management can significantly reduce dFAD beachings in Indian and Atlantic Ocean tropical tuna purse seine fisheries. en. *Biological Conservation* 254, 108939. ISSN: 0006-3207. https://doi.org/10.1016/j.biocon.2020.108939.

Imzilen T, C Lett, E Chassot, A Maufroy, M Goujon, and DM Kaplan (Apr. 2022). Recovery at sea of abandoned, lost or discarded drifting fish aggregating devices. en. *Nature Sustainability*. Publisher: Nature Publishing Group, 1–10. ISSN: 2398-9629. https://doi.org/10.1038/s41893-022-00883-y.

IOTC (2019). *Resolution 19/02 - Procedures on a Fish Aggregating Devices (FADs) Management Plan*. Tech. rep. Indian Ocean Tuna Commission.

— (2021). *Resolution 21/01 - On an intermin plan for rebuilding the Indian Ocean yellowfin tuna stock in the IOTC area of competence*. Tech. rep. Indian Ocean Tuna Commission.

— (2023a). *Resolution 23/02 on the management of drifting fish aggregating devices (DFAD) in the IOTC area of competence*. Tech. rep.

— (2023b). *Resolution 23/04 - On establishing catch limits for bigeye tuna in the IOTC area of competence*. Tech. rep. Indian Ocean Tuna Commission.

— (June 2024). *An update on the dynamics of the satellite-tracked buoys used in the large-scale purse seine fishery of the Indian Ocean, 2020-2023*. en. IOTC ad hoc Working Group on FADs (WGFAD06) IOTC-2024-WGFAD06-05. Online: Indian Ocean Tuna Commission, p. 10.

ISSF (Mar. 2023). *Status of the World Fisheries for Tuna: March 2023*. ISSF Technical Report. International Seafood Sustainability Foundation.

Jain A, L Raes, and P Manyara (2021). *Efficiency of beach clean-ups and deposit refund schemes (DRS) to avoid damages from plastic pollution on the tourism sector in Cape Town, South Africa*. Tech. rep. Switzerland: IUCN, p. 10.

Kapoor I (Nov. 2001). Towards participatory environmental management? *Journal of Environmental Management* 63, 269–279. ISSN: 0301-4797. https://doi.org/10.1006/jema.2001.0478.

Lau-Medrano W, D Gaertner, F Marsac, L Guéry, and DM Kaplan (July 2024). First look at the distribution of deactivated dFADs used by the French Indian Ocean tropical tuna purse-seine fishery. *ICES Journal of Marine Science*, fsae104. ISSN: 1054-3139. https://doi.org/10.1093/icesjms/fsae104.

Lau-Medrano W, D Gaertner, F Marsac, and DM Kaplan (May 2025). Trends and drivers of French tropical tuna purse-seine vessel behavior in the Atlantic and Indian Oceans, 2004–2020. *Fisheries Research* 285, 107330. ISSN: 0165-7836. https://doi.org/10.1016/j.fishres.2025.107330.

Lennert-Cody CE, G Moreno, V Restrepo, MH Román, and MN Maunder (Oct. 2018). Recent purse-seine FAD fishing strategies in the eastern Pacific Ocean: what is the appropriate number of FADs at sea? *ICES Journal of Marine Science* 75, 1748–1757. ISSN: 1054-3139. https://doi.org/10.1093/icesjms/fsy046.

Lindstrand N and K Thunell (2017). From Plastic to Paper Mapping the real cost of plastics. MA thesis. Stockholm, Sweden: KTH.

Lopez J, G Moreno, I Sancristobal, and J Murua (July 2014). Evolution and current state of the technology of echo-sounder buoys used by Spanish tropical tuna purse seiners in the Atlantic, Indian and Pacific Oceans. en. *Fisheries Research* 155. L, 127–137. ISSN: 0165-7836. https://doi.org/10.1016/j.fishres.2014.02.033.

Marsac F, A Fonteneau, and A Michaud (2014). *L'or bleu des Seychelles : Histoire de la pêche industrielle au thon dans l'océan Indien*.

Marsac F, A Fonteneau, and F Ménard (Jan. 2000). Drifting FADs used in tuna fisheries: an ecological trap? en. *Pêche Thonière et Dispositifs de Concentration de Poissons* 28. L, 537–552.

Martinet V and F Blanchard (Oct. 2009). Fishery externalities and biodiversity: Trade-offs between the viability of shrimp trawling and the conservation of Frigatebirds in French Guiana. *Ecological Economics* 68, 2960–2968. ISSN: 0921-8009. https://doi.org/10.1016/j.ecolecon.2009.06.012.

Maufroy A, DM Kaplan, N Bez, AD De Molina, H Murua, L Floch, and E Chassot (Jan. 2017). Massive increase in the use of drifting Fish Aggregating Devices (dFADs) by tropical tuna purse seine fisheries in the Atlantic and Indian oceans. en. *ICES Journal of Marine Science* 74. L, 215–225. ISSN: 1054-3139, 1095-9289. https://doi.org/10.1093/icesjms/fsw175.

Mittempergher D, L Raes, and A Jain (2022). *The economic impact of marine plastic pollution in Antigua and Barbuda: Impacts on the fisheries and tourism sectors, and the benefits of reducing mismanaged waste*. Tech. rep. Switzerland: IUCN.

Ortiz de Urbina J, T Brunel, R Coelho, G Merino, C Santos, H Murua, P Bach, S Saber, and D Macias (2018). *A preliminary stock assessment for the silky shark in the Indian Ocean using a data-limited approach*. en. IOTC 14th Working Party on Ecosystem and Bycatch IOTC-WPEB14-2018-033. Indian Ocean Tuna Commission.

Purves M, MS Adam, and R Bealey (2021). *A polluter pays principle for drifting FADs – how it could be applied?* IOTC Working Group on FADs (WGFAD2) IOTC-2021-WGFAD02-08. Indian Ocean Tuna Commission.

Quimby B and A Levine (Sept. 2018). Participation, Power, and Equity: Examining Three Key Social Dimensions of Fisheries Comanagement. en. *Sustainability* 10. Number: 9 Publisher: Multidisciplinary Digital Publishing Institute, 3324. ISSN: 2071-1050. https://doi.org/10.3390/su10093324.

Raes L, D Mittempergher, and A Jain (2022a). *The economic impact of marine plastic pollution in Grenada: Impacts on the fisheries and tourism sectors, and the benefits of reducing mismanaged waste*. Tech. rep. Switzerland: IUCN.

— (2022b). *The economic impact of marine plastic pollution in Saint Lucia: Impacts on the fisheries and tourism sectors, and the benefits of reducing mismanaged waste*. Tech. rep. Switzerland: IUCN.

Sanabria Garcia E and L Raes (2021). *Economic Assessment of a Deposit Refund System (DRS), an Instrument for the Implementation of a Plastics Circular Economy in Menorca, Spain*. Tech. rep. Switzerland: IUCN.

Schiller L, NG D'Costa, and B Worm (May 2025). The global footprint of drifting fish aggregating devices. *Science Advances* 11. Publisher: American Association for the Advancement of Science, eads2902. https://doi.org/10.1126/sciadv.ads2902.

Tidd A, L Dagorn, M Capello, and P Guillotreau (Feb. 2025). Overcapacity and dynamics of a tuna fleet facing catch limits and high efficiency: the case of the Indian Ocean tuna fishery. en. *Reviews in Fish Biology and Fisheries*. ISSN: 1573-5184. https://doi.org/10.1007/s11160-025-09925-y.

Tidd A, L Floc'h, T Imzilen, M Tolotti, L Dagorn, M Capello, and P Guillotreau (Oct. 2023). How technical change has boosted fish aggregation device productivity in the Indian Ocean tuna fishery. en. *Scientific Reports* 13. Publisher: Nature Publishing Group, 17834. ISSN: 2045-2322. https://doi.org/10.1038/s41598-023-45112-4.

Tolotti M, P Guillotreau, F Forget, M Capello, and L Dagorn (May 2022). Unintended effects of single-species fisheries management. en. *Environment, Development and Sustainability*. ISSN: 1573-2975. https://doi.org/10.1007/s10668-022-02432-1.

Tolotti MT, F Forget, M Capello, JD Filmalter, M Hutchinson, D Itano, K Holland, and L Dagorn (June 2020). Association dynamics of tuna and purse seine bycatch species with drifting fish aggregating devices (FADs) in the tropical eastern Atlantic Ocean. en. *Fisheries Research* 226, 105521. ISSN: 0165-7836. https://doi.org/10.1016/j.fishres.2020.105521.

Wain G, L Guéry, DM Kaplan, and D Gaertner (Feb. 2021). Quantifying the increase in fishing efficiency due to the use of drifting FADs equipped with echosounders in tropical tuna purse seine fisheries. *ICES Journal of Marine Science* 78, 235–245. ISSN: 1054-3139. https://doi.org/10.1093/icesjms/fsaa216.

Waldo S, F Jensen, M Nielsen, H Ellefsen, J Hallgrimsson, C Hammarlund, Ø Hermansen, and J Isaksen (Apr. 2016). Regulating Multiple Externalities: The Case of Nordic Fisheries. en. *Marine Resource Economics*. Publisher: University of Chicago PressChicago, IL. ISSN: 0738-1360. https://doi.org/10.1086/685286.

Walker E and N Bez (Aug. 2010). A pioneer validation of a state-space model of vessel trajectories (VMS) with observers' data. en. *Ecological Modelling* 221, 2008–2017. ISSN: 03043800. https://doi.org/10.1016/j.ecolmodel.2010.05.007.

S1 Supplementary Materials - Behavioral model

We build from the non-social (NS) model in Capello et al., 2022, but instead of working with numbers, we consider densities. Hence, we consider the total simulation area (L^2) and introduce the density of FADs noted ρ_n, the density of FADs occupied by an aggregation of size s noted ρ_s, the density of associated schools noted ρ_a and the density of free-swimming schools noted ρ_X. We also consider the following variables:

- f the proportion of occupied FADs
- m the average biomass under an occupied FAD
- n the total number of FADs. Note that $\rho_n = \frac{n}{L^2}$
- F_s the number of FADs with an aggregation of size s. Note that $\rho_s = \frac{F_s}{L^2}$
- X_1 the number of free-swimming schools of unitary size. As we consider the non-social model, X_1 also corresponds to the free-swimming population. Note that $\rho_X = \frac{X_1}{L^2}$
- N the total tuna population
- X_a the associated tuna population. Note that $\rho_a = \frac{X_a}{L^2}$
- μ the area covered by a tuna school per unit of time (in km^2.day^{-1}).
- θ the probability to leave a FAD (in day^{-1}).

S1.1 Relationship between the number of FADs and the associated population (X_a)

The time evolution of the density of FADs with an associated aggregation of size s can be expressed as:

$$\frac{1}{L^2}\frac{dX_s}{dt} = -\mu\frac{F_s X_1}{L^4} + \frac{F_{s+1}}{L^2}\theta(s+1) + \mu\frac{F_{s-1}X_1}{L^4} - \frac{F_s}{L^2}\theta s \tag{S1}$$

and, the variations of the density of free-swimming schools through time as

$$\frac{1}{L^2}\frac{dX_1}{dt} = -\mu\frac{nX_1}{L^4} + \sum_{s=1}^{N} s\theta\frac{F_s}{L^2} \tag{S2}$$

We consider that the system is at equilibrium, so we have $\frac{dX_s}{dt} = \frac{dX_1}{dt} = 0$. Hence

$$X_1 = \frac{\theta L^2}{\mu n}\sum_{s=1}^{N} sF_s = \frac{\theta L^2}{\mu n}X_a$$

Moreover, we have conservation of the population ($N = X_a + X_1$). So

$$\begin{aligned} N &= X_a\left(1 + \frac{\theta L^2}{\mu n}\right) \\ \Leftrightarrow X_a &= N\frac{\mu n}{\mu n + \theta L^2} \end{aligned} \tag{S3}$$

S1.2 Relationship between the number of FADs and the fraction of FADs that are occupied by tuna (f)

We have

$$f = \frac{n - F_0}{n} \tag{S4}$$

and

$$n = F_0 + \sum_{s=1}^{N} F_s \tag{S5}$$

S1.2.1 Determination of F_s

At equilibrium, we want to demonstrate that

$$F_s = \frac{1}{s!}\Big(\frac{\mu X_1}{\theta L^2}\Big)^s F_0$$

1. Expression of F_1

$$\begin{aligned} 0 &= -\mu\frac{F_0 X_1}{L^4} + \frac{F_1}{L^2}\theta \\ \Leftrightarrow F_1 &= \frac{\mu X_1}{\theta L^2} F_0 \\ \Leftrightarrow F_1 &= \frac{1}{1!}\Big(\frac{\mu X_1}{\theta L^2}\Big)^1 F_0 \end{aligned}$$

2. Expression of F_2

$$\begin{aligned} 0 &= -\mu\frac{F_1 X_1}{L^4} + 2\frac{F_2}{L^2}\theta + \mu\frac{F_0 X_1}{L^4} - \frac{F_1}{L^2}\theta \\ \Leftrightarrow \quad 0 &= -\mu\frac{F_1 X_1}{L^4} + 2\frac{F_2}{L^2}\theta \\ \Leftrightarrow \quad F_2 &= \frac{1}{2}\frac{\mu X_1}{\theta L^2} F_1 \\ \Leftrightarrow \quad F_2 &= \frac{1}{2}\Big(\frac{\mu X_1}{\theta L^2}\Big)^2 F_0 \end{aligned}$$

3. Expression of F_{s+1}

$$\begin{aligned} 0 &= -\mu\frac{F_s X_1}{L^4} + \frac{F_{s+1}}{L^2}\theta(s+1) + \mu\frac{F_{s-1} X_1}{L^4} - \frac{F_s}{L^2}\theta s \\ \Leftrightarrow \quad F_{s+1}\theta(s+1) &= \mu\frac{F_s X_1}{L^2} + F_s\theta s - \mu\frac{F_{s-1} X_1}{L^2} \\ \Leftrightarrow \quad F_{s+1} &= \frac{\mu}{\theta(s+1)L^2} F_s X_1 + F_s\frac{s}{s+1} - \frac{\mu}{\theta(s+1)L^2} F_{s-1} X_1 \\ \Leftrightarrow \quad F_{s+1} &= \frac{\mu}{\theta L^2(s+1)} X_1 \frac{1}{s!}\Big(\frac{\mu X_1}{\theta L^2}\Big)^s F_0 + \frac{1}{s!}\Big(\frac{\mu X_1}{\theta L^2}\Big)^s F_0\frac{s}{s+1} - \frac{\mu}{\theta L^2(s+1)} X_1 \frac{1}{(s-1)!}\Big(\frac{\mu X_1}{\theta L^2}\Big)^{s-1} F_0 \\ \Leftrightarrow \quad F_{s+1} &= \frac{1}{(s+1)}\frac{1}{s!}\Big(\frac{\mu X_1}{\theta L^2}\Big)^{s+1} F_0 + \frac{1}{(s-1)!}\Big(\frac{\mu X_1}{\theta L^2}\Big)^s F_0\frac{1}{s+1} - \frac{1}{(s+1)}\frac{1}{(s-1)!}\Big(\frac{\mu X_1}{\theta L^2}\Big)^s F_0 \\ \Leftrightarrow \quad F_{s+1} &= \frac{1}{(s+1)}\frac{1}{s!}\Big(\frac{\mu X_1}{\theta L^2}\Big)^{s+1} F_0 \end{aligned}$$

Hence, we have

$$F_s = \frac{1}{s!}\Big(\frac{\mu X_1}{\theta L^2}\Big)^s F_0 \tag{S6}$$

S1.2.2 Determination of f

From Eq. S5 and S6, we have

$$\begin{aligned} & n = F_0 + \sum_{s=1}^{N} F_s \\ \Leftrightarrow \quad & n = F_0 + \sum_{s=1}^{N} \frac{1}{s!}\left(\frac{\mu X_1}{\theta L^2}\right)^s F_0 \\ \Leftrightarrow \quad & F_0 = \frac{n}{1 + \sum_{s=1}^{N} \frac{1}{s!}\left(\frac{\mu X_1}{\theta L^2}\right)^s} \\ \Leftrightarrow \quad & F_0 = \frac{n}{\sum_{s=0}^{N} \frac{1}{s!}\left(\frac{\mu X_1}{\theta L^2}\right)^s} \end{aligned}$$

Also

$$f = \frac{n - F_0}{n} = 1 - \frac{F_0}{n} \tag{S7}$$

So

$$f = 1 - \frac{1}{\sum_{s=0}^{N} \frac{1}{s!}\left(\frac{\mu X_1}{\theta L^2}\right)^s}$$

Moreover

$$\begin{aligned} & X_1 = \frac{\theta L^2 X_a}{\mu n} \\ \Leftrightarrow \quad & X_1 = \frac{\theta L^2}{\mu n} N \frac{\mu n}{\mu n + \theta L^2} \\ \Leftrightarrow \quad & X_1 = \frac{\theta L^2 N}{\mu n + \theta L^2} \end{aligned}$$

So

$$f = 1 - \frac{1}{\sum_{s=0}^{N} \frac{1}{s!}\left(\frac{\mu N}{\mu n + \theta L^2}\right)^s} \tag{S8}$$

S1.3 Relationship between the number of FADs and the average biomass under an occupied FAD (m)

We have

$$m = \frac{\rho_a}{\rho_n f} = \frac{X_a}{nf}$$

Hence

$$m = \frac{N\mu}{(\mu n + \theta L^2) f} \tag{S9}$$

S1.4 Relationship between the number of FADs and the aggregation Continuous Absence and Residence Times (aCAT and aCRT)

We have

$$\text{aCAT} = \frac{1}{\mu\rho_X} = \frac{L^2}{\mu X_1} = \frac{\mu n + \theta L^2}{\mu\theta N} \tag{S10}$$

Also

$$f = \frac{\text{aCRT}}{\text{aCAT} + \text{aCRT}} \tag{S11}$$

$$\Leftrightarrow \quad f(\text{aCAT} + \text{aCRT}) = \text{aCRT}$$

$$\Leftrightarrow \quad f\text{aCAT} = \text{aCRT}(1 - f)$$

$$\Leftrightarrow \quad \text{aCRT} = \text{aCAT}\frac{f}{1 - f} \tag{S12}$$

S1.5 Implementing the relationships in the model

S1.5.1 aCRT, aCAT and m values determination for tuna

First, using Eq. S11 and aCAT and aCRT values from Baidai et al., 2020b algorithm (see Section 2.1.1 in main manuscript), we determined the current f value in the western Indian Ocean. We found $f = 0.272$. Then, using Eq. S8, we determined the value of N such that $f = 0.272$. Other parameter values were determined as follow:

- n = 12,000, the total number of FADs in the simulations and L = 1,200 km, both chosen to correspond to the maximum observed DFAD density in the western Indian Ocean in Dupaix, Dagorn, et al., 2024 (density of 8.3×10^{-3} km^{-2}).

- $\mu = 24.14$ km^2.day^{-1}.
  We consider $X(t = 0)$ the density of tuna schools leaving a FAD at $t = 0$ and $X(t)$ the density of schools that left a FAD at $t = 0$ and are still free-swimming at time t. We consider $x(t) = \frac{X(t)}{X(0)}$ then $\frac{dx(t)}{dt} = -X(t)k(t)$.
  We consider k to be constant and proportional to the surface explored by a tuna during a day (μ, in km^2.day^{-1}) and to the density of FADs ($\frac{n}{L^2}$, in km^{-2}).
  Then $x(t) = e^{-kt}$ with $k = \frac{n\mu}{L^2}$.
  k is the rate at which tuna schools associate, which is the inverse of the average time between two associations, meaning that $k = \frac{1}{\text{CAT}}$.
  Hence, we have
  $\mu = \frac{L^2}{n\text{CAT}}$.
  From Dupaix, Dagorn, et al., 2024, the average CAT value for YFT in the western Indian Ocean is CAT = 4.97 days.

- $\theta = 0.15$ day^{-1}. From Govinden et al., 2021, the average CRT value for YFT in the western Indian Ocean is CRT = 6.64 days. Hence, $\theta = \frac{1}{\text{CRT}} = 0.15$ day^{-1}.

From these parameter values, we determined f (Eq. S8), m (Eq. S9), aCAT (Eq. S10) and aCRT (Eq. S12) values for n values tested in the simulations (Figure S1).

S1.5.2 m values determination for silky sharks

Using Eq. S9, we determined m_{SLK} as a function of the number of FADs n, with the following parameter values:

- n = 12,000, the total number of FADs in the simulations and L = 1,200 km, both chosen to correspond to the maximum observed DFAD density in the western Indian Ocean in Dupaix, Dagorn, et al., 2024 (density of 8.3×10^{-3} km^{-2}).
- N_{SLK} = 403,920 metric tons, from the preliminary stock assessment performed in the Indian Ocean (Ortiz de Urbina et al., 2018).
- $\mu_{SLK} = \frac{L^2}{n\text{CAT}_{SLK}} = 59.41$ km^2.day^{-1}, with the average CAT of silky shark in the Western Indian Ocean $\text{CAT}_{SLK} = 2.02$ days (MT Tolotti et al., 2020).
- $\theta_{SLK} = 0.17$ day^{-1}, with the average CRT value for silky shark in the Indian Ocean of CRT = 5.90 days (MT Tolotti et al., 2020).
- $f = 1$, in the absence of aCRT and aCAT values, and considering Eq S8.

The obtained values, expressed in number of schools of silky sharks, were multiplied by the ratio of the average number of silky sharks caught per set in the Western Indian Ocean ($m_{SLK} = 8.26$) (M Tolotti et al., 2022) and of the value obtained with n = 12,000 (Figure S3).

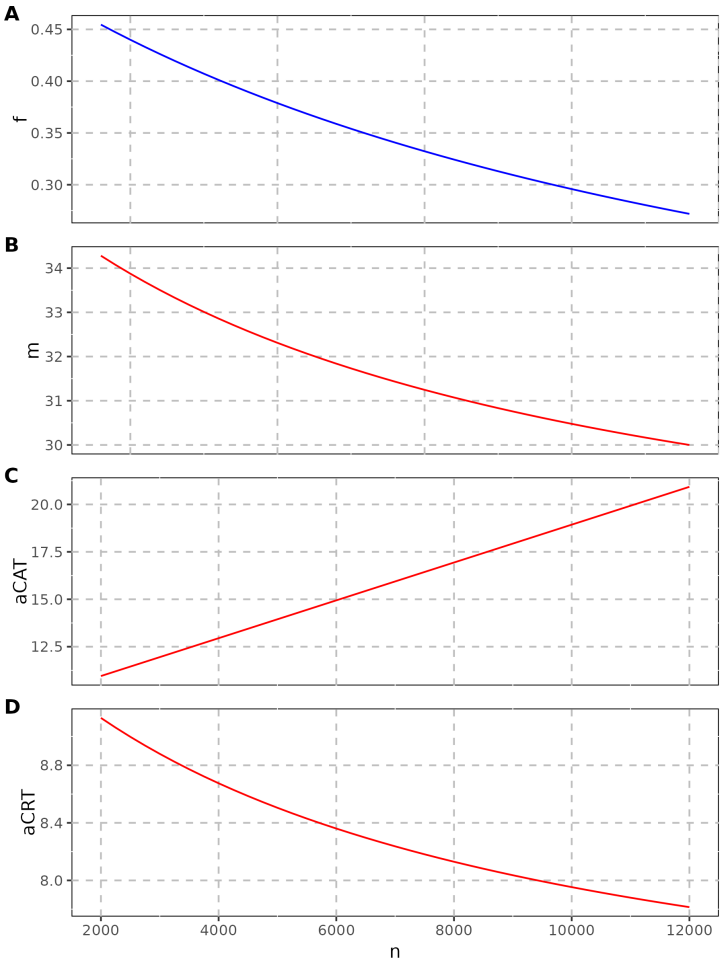

Figure S1. Modelling tuna associative behavior. (A) Fraction of occupied FADs f as a function of the number of FADs n **(B)** Average biomass under occupied FADs m in metric tons, corresponding to the average catch-per-set **(C)** Average aggregation Continuous Absence Time (aCAT) in days, defined as the period between two consecutive detections of tuna aggregations at the same FAD, and **(D** Average aggregation Continuous Residence Time (aCRT) in days, defined as the time span within which a tuna aggregation is continuously detected at a FAD without a day scale ($>$24 h) absence. Relationships were obtained considering a non-social scenario and using a random forest algorithm and echosounder buoys data for calibration **methods**; Baidai et al., 2020a,b; Capello et al., 2022.

S2 Supplementary Materials

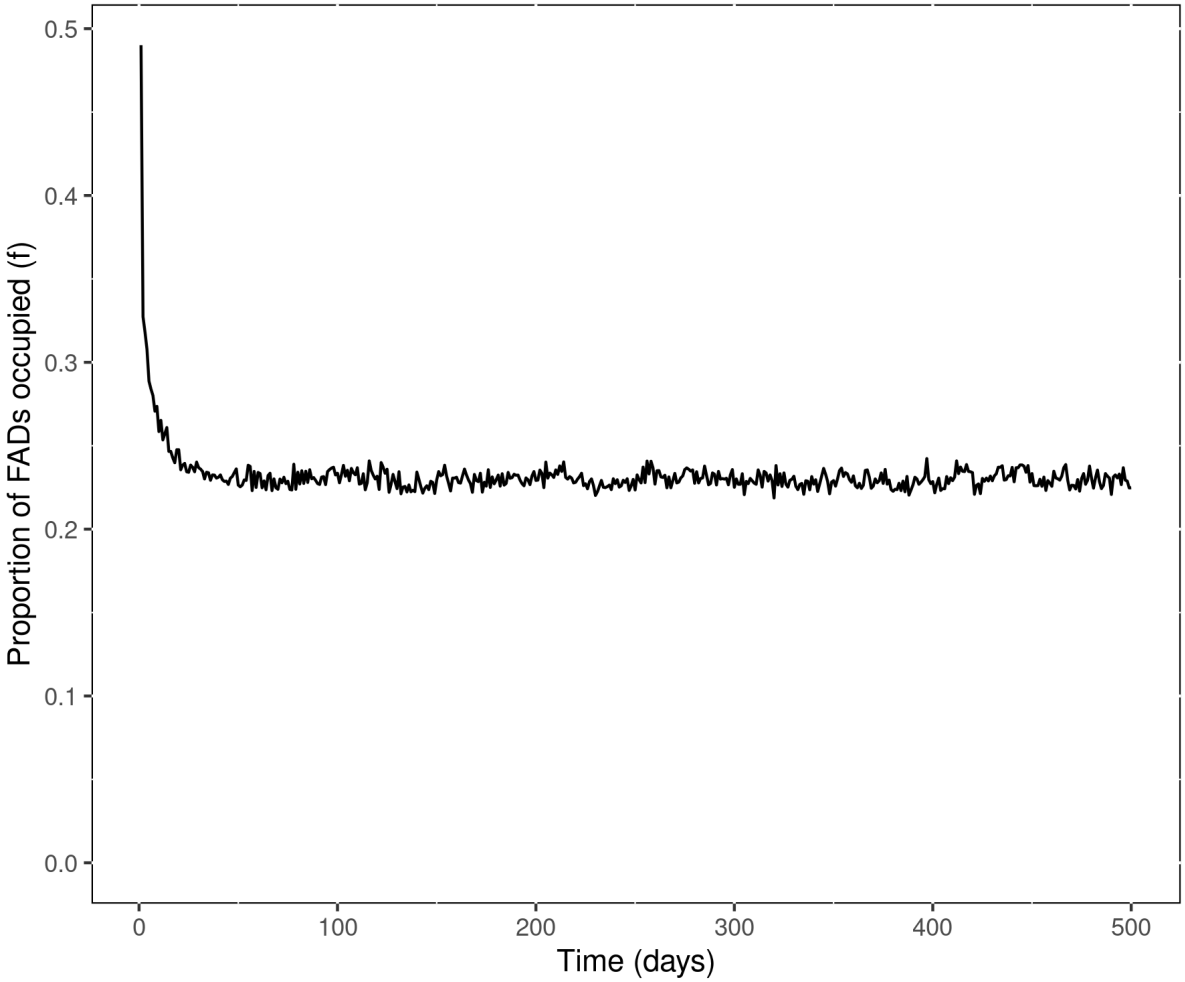

Figure S2. Proportion of FADs occupied by tuna in the model (noted f). Values were obtained simulating a FAD array of 1000 FADs, during 500 days with no fishing vessel.

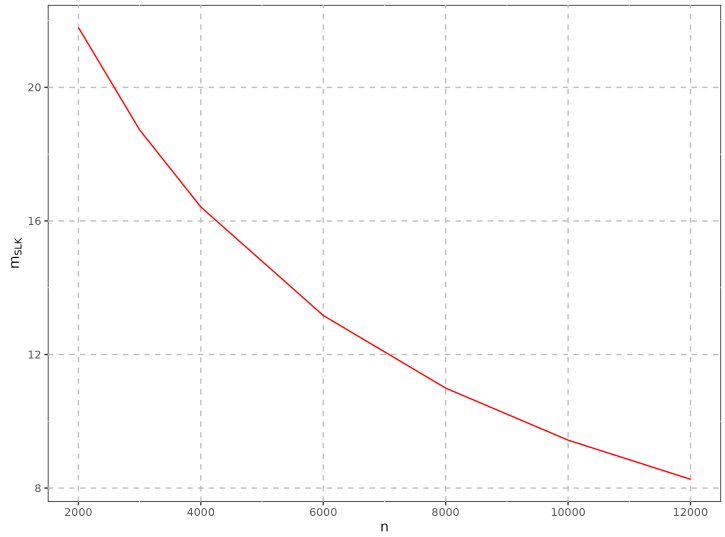

Figure S3. Variations of silky shark catch-per-set as a function of the number of FADs n (in numbers).